Check for updates

The rapid response and high sensitivity of a ruthenium-doped copper ferrite thin film (Ru–CuFe$_2$O$_4$) sensor

V. Manikandan, [ID] *[a] Ali Mirzaei,[b] S. Sikarwar,[c] B. C. Yadav, [ID] [c] S. Vigneselvan,[d] A. Vanitha[d] and J. Chandrasekaran[e]

A sensor displaying a rapid response and high sensitivity was developed by following a simple route. Ionic defects in this sensor were explored using X-ray diffraction analysis. In general, such defects arise from a mismatch of ionic radii, which actually improves the sensing performance. SEM and TEM images of the currently produced particles demonstrated negligible agglomeration, which greatly enhanced the flow of water molecules through the particles. The current sensor showed a rapid response to changes in humidity. Its sensing performance was classified into three different ranges of humidity. Of these humidity ranges, the sensor showed the highest sensitivity (8.84 MΩ per %RH) at low relative humidity (10–20% RH). Furthermore, the sensitivity fall off as the RH was increased from 20 to 99%. The sensor showed a rapid response time of 20 s. Also, the sensor showed 92.98% reproducibility and few effects of aging.

1. Introduction

Precise determination of humidity levels is essential in the fields of climate forecasting, food storage, motor industries, textiles, chemical industries and agriculture, and thus the fabrication of a rapidly responsive humidity sensor has garnered very considerable interest.[1] In particular, the development and use of sensors that are highly sensitive to low relative humidity environments is very important for effectively monitoring ultra-clean chambers, chemical storage units, integrated chips, and manufacturing units.[2] And rapid-response sensors can be used to precisely determine relative humidity values at the low relative humidity range. In this regard, a focus must be made on finding highly potent nanomaterials for the fabrication of rapid-response humidity sensors.[3,4] Most humidity sensors are based either on resistance or capacitance. The adsorption of water molecules on the nanomaterial surface is reflected in an impedance or dielectric constant change.[5] In contrast to capacitive-based sensors, resistance-based sensors display robust responses and other potential features including long-duration performance and the ability to mass produce them economically.[6] Nanoscale ferrites are, due to their diverse applications, presently being investigated for use in sensors of relative humidity. To produce powerful rapid-response sensors of relative humidity, the properties of the sensor may need to be tuned *via* changing characteristics of the sensor material, such as its composition, crystallite size, porosity and shape[7]. Copper ferrite nanoparticles have enhanced humidity-sensing properties at room temperature.[8] In addition, the nanoparticles are stable to chemical and thermal treatments. And they offer a sufficient surface-to-volume ratio for interaction with water molecules.[9] The sensing ability of the copper ferrite nanoparticles can be enhanced by adjusting their surface areas, morphologies and particle sizes, features that can be affected by doping.[10,11] Ruthenium is an effective dopant and displays good electrical conductivity.[12] It can enhance the response to humidity and increase the sensitivity of a sensor. To the best of our knowledge, a ruthenium-doped copper ferrite thin film humidity sensor has not been reported so far. Ruthenium could substitute for iron in iron sites, with interactions between these ions leading to iron defects.[13,14] The iron defects can be termed as Fe$_2$O$_3$ secondary phases, which have been shown to increase surface-to-volume ratios. Increasing surface area has been shown to directly lead to increased impacts on sensing.[15]

The objective of the current work was to enhance sensitivity and response time to low relative humidity. The prepared ruthenium-doped copper ferrite thin film sensor was examined for different ranges of relative humidity. An overall test showed the sensor displaying a rapid response and high sensitivity at

[a]Department of Physics, Kongunadu Arts and Science College, Coimbatore-641 029, India. E-mail: manikandan570@gmail.com

[b]Department of Materials Science and Engineering, Shiraz University of Technology, Shiraz, Iran

[c]Nanomaterials and Sensors Research Laboratory, Department of Physics, Babasaheb Bhimrao University, Lucknow-226 025, UP, India

[d]Department of Physics, Government College of Technology, Coimbatore-641 013, India

[e]Department of Physics, Sri Ramakrishna Mission Vidyalaya College of Arts & Science, Coimbatore-641 020, India

low relative humidity. In a narrow humidity detection range, the sensor displayed the highest sensitivity of reported sensors and negligible aging effects. A comparison of parameters of the present sensor with those of previously reported sensors is shown in Table 1.

2. Experimental details

Ruthenium-doped copper ferrite was prepared by following the chemical co-precipitation method using an aqueous solution, specifically using de-ionized water. The concentrations of the elements were chosen to realize the chemical formula Ru_x-$CuFe_{2-x}O4$ ($x = 0.2$). In the synthesis, analytical grade $CuCl_2\cdot 2H_2O$, $FeCl_3\cdot 9H_2O$, $RuCl_3\cdot 2H_2O$ and NaOH were dissolved in 100 mL of de-ionized water to form a brown-colored solution, which was stirred for 2 h until a dark brown precipitate formed. The precipitate was dried at 150 °C for 24 h and then subjected to a heat treatment at 900 °C for 4 h in a silica crucible. A borosilicate substrate with dimensions of 1.5×1.5 cm^2 was ultrasonically washed and then dried at 150 °C. The above-obtained ruthenium-doped copper ferrite fine powder was spin-coated on the substrate with a revolution rate of 500 min^{-1} and thin films were obtained. The thickness of the film was 15 μm. Note that borosilicate substrates were used since they are in general the most cost-effective substrates, and since they are highly resistant to most substances and have superior chemical resistance to most metals and other materials even when exposed for prolonged periods of time at high temperatures. Silver contacts were made on the two ends of the film, which were used as electrodes. Furthermore, the film was kept inside a humidity-controlled chamber and was then heated for 15 min to completely dry it. Then, the connecting wires were used to make contact between the electrodes and the impedance analyzer, a concentrated aqueous solution of K_2SO_4 was placed in the humidity-controlled chamber, and then the chamber was sealed. Then the humidity was increased, and the impedance of the film was measured and plotted. In this way, the film was employed as a sensor.

2.1 Characterization

X-ray diffraction (XRD, Rigaku) using Cu Kα$_1$ radiation with a wavelength of 1.5406 Å was used to explore the crystallinity of the synthesized material. The thickness of the film was measured using a surface profilometer. The morphologies of
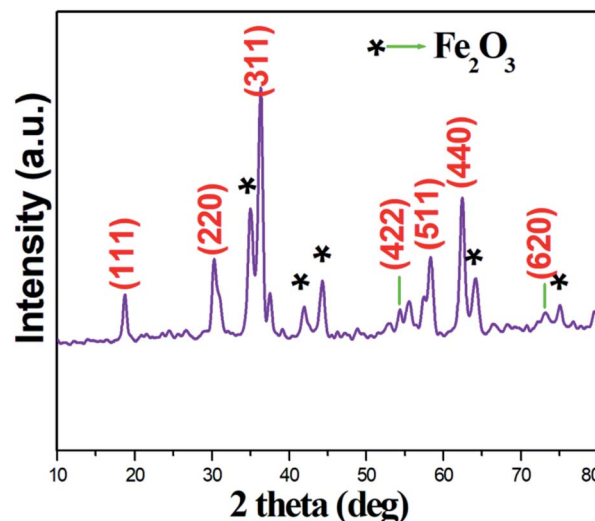
Table 1 Parameters of the present sensor and of previously reported ones

S. no	Material	%RH range	Sensitivity	Ref.
1	ZrO_2	20–40	∼1.52 MΩ per %RH	16
2	In–SnO_2	20–45	0.0066 MΩ per %RH	1
3	$NaNbO_3$	10–20	0.086 MΩ per %RH	6
4	$ZnSb_2O_4$	10–20	0.0056 MΩ per %RH	17
5	Sn–$NiFe_2O_4$	10–35	2.08 MΩ per %RH	18
6	Li–$CuFe_2O_4$	10–30	5.90 MΩ per %RH	19
7	Ru–$CuFe_2O_4$	10–20	8.84 MΩ per %RH	Present work

Fig. 1 XRD pattern of Ru–$CuFe_2O_4$.

the products were studied using scanning electron microscopy (SEM, JEOL 5600 V; 10 kV operating voltage) and the microstructure by using transmission electron microscopy (TEM; Phillips CM-200). Energy-dispersive X-ray analysis (EDX) was carried out using an X-ray analyzer coupled with the TEM. A humidity sensing test was performed by using an impedance analyzer (Wayne Kerr Precision Component Analyzer, 6440B).

2.2 Humidity sensing tests

The set-up used for humidity sensing had a glass chamber whose humidity could be controlled. The fabricated Ru-doped copper ferrite thin film using silver electrodes was fixed into the humidity chamber and then interfaced with an impedance analyzer (Wayne Kerr Precision Component Analyzer, 6440B). Humidification and dehumidification were effected using saturated aqueous solutions of K_2SO_4 and KOH. Relative

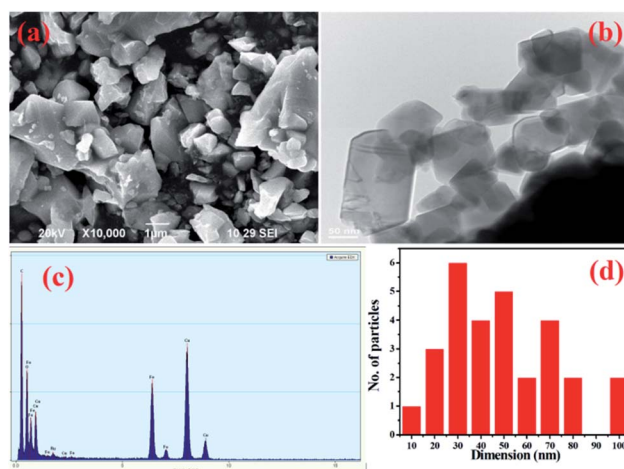**Fig. 2** (a) SEM, (b) TEM, and (c) EDX images and (d) the particle size distribution of the Ru–$CuFe_2O_4$ thin film.
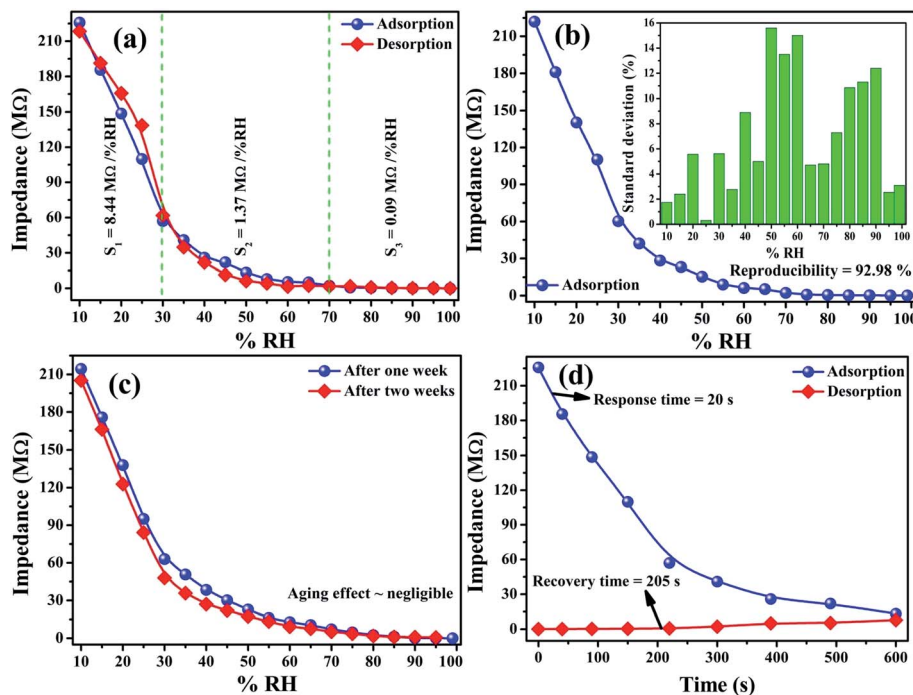
Fig. 3 Sensing performance of the Ru–CuFe$_2$O$_4$ sensor showing (a) sensing response, (b) reproducibility, (c) aging effects and (d) response/recovery time.

humidity was monitored using a standard hygrometer (HTC-1). Changes were recorded in the electrical impedance of sensor as the relative humidity (RH) was changed in the range 10–99%. All sensing tests were performed at room temperature. During the humidity tests, impedance decreased with increasing %RH and sensitivity was calculated using eqn (1).

$$\text{Sensitivity} = \frac{\text{change in an impedance } (\Delta I)}{\text{corresponding change in the \%RH } (\Delta \%RH)} \quad (1)$$

3. Results and discussion

Powder X-ray spectra of the Ru-doped copper ferrite thin film showed peaks corresponding to various diffraction planes, specifically (111), (220), (422), (511), (440), and (620) (Fig. 1), and indicated a face-centered cubic crystal structure with the *Fd3m* space group, which were identified by a comparison of the spectra with JCPDS card #77-0010. As well as these diffraction planes, secondary phase (Fe$_2$O$_3$) diffraction planes are noticed, and are denoted as ionic defects. The defects may have been located at sublattices. However, the impairment of ferromagnetic resonance causes the development of ionic defects.[20] In this sense, the exchange energy between unpaired electron spins from different orbitals seed ionic defects.[21] Such ionic defects would result in more surfaces for adsorption/desorption of water molecules. The crystallite size of the synthesized material was calculated from the very intense (311) diffraction peak to be ∼24 nm. Ruthenium ions are bigger than iron ions, and this mismatch would facilitate a lattice expansion.[22] The

lattice expansion assists the diffusion of oxygen, which would promote the adsorption/desorption of water molecules.[23]

The SEM image acquired of the synthesized particles showed them displaying relatively irregular shapes and a variety of sizes (Fig. 2a). The TEM image acquired of the nanoparticles showed cylindrical and square shapes with negligible agglomeration (Fig. 2b). In general in ferrite systems, agglomerations of nanoparticles are highly possible, but the prepared material showed less contact with neighboring particles than is generally observed. Less agglomeration would be expected to create relatively unimpeded paths through which water molecules can more easily flow. An acquired EDX spectrum of the material is shown in Fig. 2c; analysis of this spectrum indicated the presence of oxygen, copper, iron and ruthenium in the required ratio. A particle size distribution histogram of the Ru-doped copper ferrite thin film is shown in Fig. 3d. Inspection of this histogram indicated particle sizes between 20–50 nm and 60–80 nm. This first range of particle sizes (20–50 nm) was consistent with the analysis of the XRD results.

Fig. 3a shows sensing curves of adsorption and desorption (impedance *versus* %RH) for the Ru-doped copper ferrite thin film during injection and removal of humidity (hysteresis test).

Table 2 Sensitivity values of the Ru-doped copper ferrite film for several %RH ranges

Humidity range	10–20 %RH	20–70 %RH	70–99 %RH
Sensitivity (3.40 MΩ per %RH)	8.44	1.37	0.09

Table 3 Sensor parameters of the Ru-doped copper ferrite thin film humidity sensor

Sensor parameter	Sensitivity	Reproducibility	Response time	Recovery time	Ageing effect
Value	3.40 MΩ per %RH	92.98%	20 s	205 s	∼7%

The %RH was increased from 10 to 99% and then decreased from 99 to 10%. The Ru-doped copper ferrite sensor showed high sensitivity in the 10–20% RH range, with a peak sensitivity here of 8.84 MΩ per RH%. But as the humidity was increased in the range 20–99% RH, the sensitivity decreased abruptly, down to 1.37 MΩ per RH% in the 20–70% RH range, and to a negligible 0.09 MΩ per RH% value at 70–99% RH. That is, its sensitivity was very poor in the 20–99% RH range. From the observations of humidity detection, the sensor shows higher sensitivity than previously reported sensors in the narrow range of 10–20% RH. The overall sensitivity of the sensor was 3.40 MΩ per %RH.[24] Sensitivity values for several %RH ranges are shown in Table 2.

The humidity sensing tests were repeated and the results are shown in Fig. 3b. The sensor achieved a 92.98% reproducibility. The standard deviation is shown in the inset of Fig. 3b. This standard deviation figure showed that the sensor was quite reproducible in the less humid range and it is less reproducible in the mid-humidity range.[24] The stability of the fabricated sensor was studied by testing it one and two weeks after it was made, and the results are presented in Fig. 3c. The sensing curves nearly overlapped, demonstrating the good stability of sensor and not much of an effect of ageing. Response and recovery times are indispensable parameters for judging the effectiveness of the sensor. As shown in Fig. 3d, the response and recovery times of the currently fabricated humidity sensor

were measured to be 20 and 205 s, respectively; these values corresponded to adsorption and desorption, respectively. The sensor showed very fast dynamics for humidity sensing.

Based on the various sensor parameters obtained for the Ru-doped copper ferrite thin film, as listed in Table 3, this sensor showed effective performance for humidity sensing. The effective sensing of humidity was due to iron defects, namely from the Fe_2O_3 phase evolution. These defects contributed an increased surface area, a feature highly desirable for adsorption and desorption of water molecules. SEM and TEM images showed the porous nature of the material, another feature apt to increase sensitivity.

Sensing mechanism

A mechanism for the humidity sensing has been proposed, as outlined in Fig. 4.[25,26]

According to this proposed mechanism, when humid air is injected into a humidity chamber, a few water molecules would become adsorbed on the surface of sensor. Due to the polar nature of the water molecule, the (negatively) charged oxygen of the water molecule can be attracted electrostatically to the (positively) charged cationic side of the metal oxide surface. In this progression, an electrostatic force would become established and lead to a chemical bonding between the water molecules and surface of the sensor. Thus a so-called
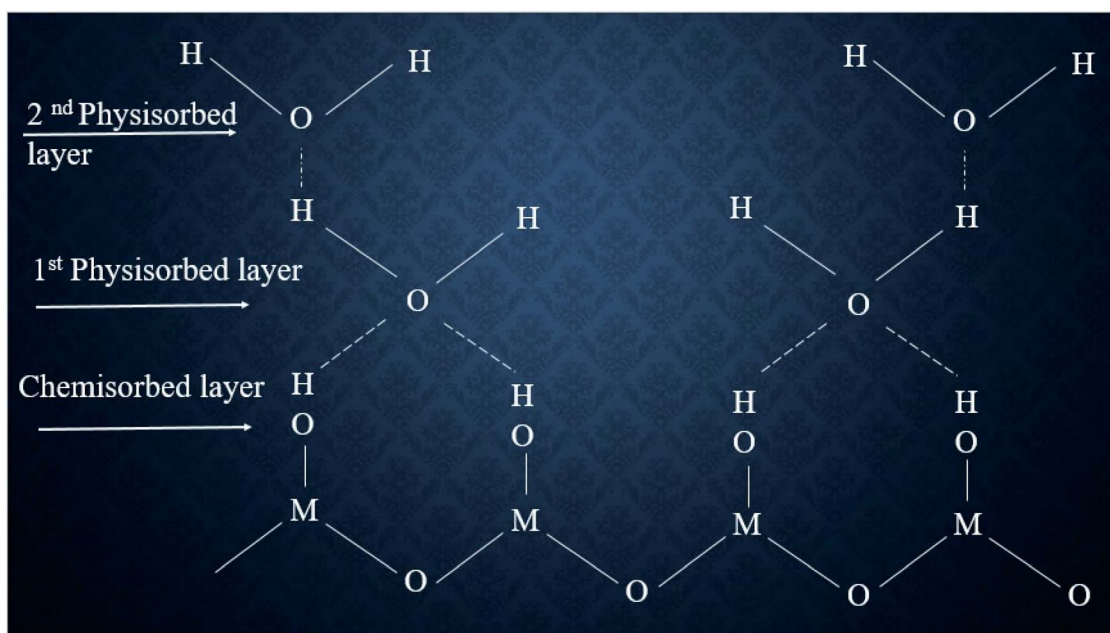
Fig. 4 The multilayer structure of adsorbed water vapor molecules on the surface of a humidity sensor.

chemisorbed layer would appearing on the surface of the sensor. The reaction for the chemisorbed layer is shown in eqn (2).[27]

$$M^+ + H_2O \rightarrow M - OH + H^+ \qquad (2)$$
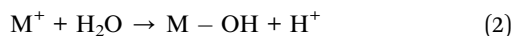
According to mechanism, the chemisorbed layer would be the first formed layer and these layers cannot be reformed due to the injection of humidity. Then water molecules would dissociate to form hydroxyl groups, which would subsequently adsorb onto metal cations, which have high charge carrier density and strong electrostatic fields. Accordingly, they would provide mobile protons. The protons would migrate on the surface and react with the neighbor surface O^{2-} species to form a second hydroxyl (OH^-) group. During the second stage, water vapor layers would become physisorbed on the first formed hydroxyl layer. In fact, the additional layer cannot form sturdy chemical bonds but can surely adsorb onto the surface of the sensing element using weak van der Waals forces. As water molecules continue to adsorb on the surface, extra layers would form on the previously formed layers and a multilayer structure would in this way form. Therefore, singly bonded water vapor molecules would become mobile and able to form continuous dipoles and electrolyte layers between the electrodes, resulting in a decrease in the resistance of the humidity sensor.[28] The high sensitivity obtained in this study may have been related to the sizes of the nanoparticles and the relatively low extent of agglomeration, features providing more adsorption sites for water molecules.

4. Conclusions

A ruthenium-doped copper ferrite thin film sensor was obtained using a simple chemical method. The thin film was observed to display relatively large crystallites, with dimensions of ~24 nm. Also, diffraction peaks attributed to ionic defects were noticed from X-ray diffraction analysis. Inspection of SEM and TEM images of this film showed a glossy surface with nanoparticles forming a variety of shapes and undergoing relatively little agglomeration. The sensor was found to be highly potent at low relative humidity. At low relative humidity (10–20 %RH), the sensor showed an ultra-high sensitivity of 8.84 MΩ per %RH and response time of 20 s. In overall testing, the sensor showed a sensitivity of 3.40 MΩ per %RH.

Conflicts of interest

The authors declare that there are no conflicts of interest.

References

1 R. Malik, V. K. Tomer, V. Chaudhary, M. S. Dahiya, A. Sharma, S. P. Nehra, S. Duhan and K. Kailasam, *J. Mater. Chem. A*, 2017, **5**, 14134–14143.

2 N. Li, X. Chen, X. Chen, X. Ding and X. Zhao, *RSC Adv.*, 2017, **7**, 45988–45996.

3 K. Ketpang, K. Lee and S. Shanmugam, *ACS Appl. Mater. Interfaces*, 2014, **6**, 16734–16744.

4 X. Liang, F. Zhang, W. Feng, X. Zou, C. Zhao, H. Na, C. Liu, F. Sun and G. Zhu, *Chem. Sci.*, 2013, **4**, 983–992.

5 Z. Ahmad, M. H. Sayyad, M. Saleem, K. S. Karimov and M. Shah, *Phys. E*, 2008, **41**, 18–22.

6 Y. Zhang, X. Pan, Z. Wang, Y. Hu, X. Zhou, Z. Hu and H. Gu, *RSC Adv.*, 2015, **5**, 20453–20458.

7 Y. Kumar, A. Sharma and P. M. Shirage, *RSC Adv.*, 2017, **7**, 55778–55785.

8 S. Muthurani, M. Balaji, S. Gautam, K. H. Chae, J. H. Song, D. P. Padiyan and K. Asokan, *J. Nanosci. Nanotechnol.*, 2011, **11**, 5850–5855.

9 A. Sharma, Y. Kumar, K. Mazumder, A. K. Rana and P. M. Shirage, *New J. Chem.*, 2018, **42**, 8445–8457.

10 S. Barth, F. Hernandez-Ramirez, J. D. Holmes and A. Romano-Rodriguez, *Prog. Mater. Sci.*, 2010, **55**, 563–627.

11 L. Han, J. Liu, Z. Wang, K. Zhang, H. Luo, B. Xu, X. Zou, X. Zheng, B. Ye and X. Yu, *CrystEngComm*, 2012, **14**, 3380–3386.

12 K. E. Swider, C. I. Merzbacher, P. L. Hagans and D. R. Rolison, *Chem. Mater.*, 1997, **9**, 1248–1255.

13 X. Jiang, W. Wang, Z. Yu, K. Sun, Z. Lan, X. Zhang and V. G. Harris, *AIP Adv.*, 2017, **7**, 056106.

14 A. Iglesias, J. Balmaseda and A. González Arias, *J. Mater. Res.*, 2002, **17**, 1702–1705.

15 R. Chen, M. G. Christiansen, A. Sourakov, A. Mohr, Y. Matsumoto, S. Okada, A. Jasanoff and P. Anikeeva, *Nano Lett.*, 2016, **16**, 1345–1351.

16 Y. Lu, Z. Wang, S. Yuan, L. Shi, Y. Zhao and W. Deng, *RSC Adv.*, 2013, **3**, 11707–11714.

17 M. Zhong, Z. Wei, X. Meng, F. Wu and J. Li, *RSC Adv.*, 2015, **5**, 2429–2433.

18 V. Manikandan, S. Sikarwar, B. C. Yadav and R. S. Mane, *Sens. Actuators, A*, 2018, **272**, 267–273.

19 V. Manikandan, S. Sikarwar, B. C. Yadav, S. Vigneselvan, R. S. Mane, J. Chandrasekaran and A. Mirzaei, *Mater. Chem. Phys.*, 2019, **229**, 448–452.

20 A. Gonzalez Arias, A. del Cueto, J. Munoz and C. de Francisco, *Mater. Lett.*, 1998, **37**, 187–191.

21 J. H. Van Vleck, *Physica*, 1951, **17**, 234–252.

22 B. Vasile, A. Mirzaei, I. Petrila, V. Kuncser, F. Tudorache, D. Morgan, R. S. Mane, S. Vigneselvan and V. Manikandan, *J. Magn. Magn. Mater.*, 2018, **474**, 563–569.

23 E. Poonia, P. K. Mishra, V. Kiran, J. Sangwan, R. Kumar, P. K. Rai, R. Malik, V. K. Tomer, R. Ahuja and Y. K. Mishra, *J. Mater. Chem. C*, 2019, **7**, 5477–5487.

24 S. Sikarwar, B. C. Yadav, R. K. Sonker, G. I. Dzhardimalieva and J. K. Rajput, *Appl. Surf. Sci.*, 2019, **479**, 326–333.

25 L. Almar, A. Tarancón, T. Andreu, M. Torrell, Y. Hu, G. Dezanneau and A. Morata, *Sens. Actuators, B*, 2015, **216**, 41–48.

26 H. Farahani, R. Wagiran and M. N. Hamidon, Humidity sensors principle, mechanism, and fabrication technologies: a comprehensive review, *Sensors*, 2014, **14**, 7881–7939.

27 S. Sikarwar and B. C. Yadav, *Sens. Actuators, A*, 2015, **233**, 54–70.

28 D. Burman, R. Ghosh, S. Santra and P. K. Guha, *RSC Adv.*, 2016, **6**, 57424–57433.